Comparative analysis of Euler models of multiphase flows in the ANSYS software for the problem of spraying raw materials in a heat-carrier gas flow in the furnace production of carbon black

Daniel Tarraf [1] and *Sergey* Cherny [2]

[1] Novosibirsk State University (NSU), 630090, Novosibirsk, Russia
[2] Kutateladze Institute of Thermophysics, 630090, Novosibirsk, Russia

Abstract. Carbon black (soot) is a product obtained by thermal decomposition (pyrolysis) of hydrocarbons (usually oil) in a heat-carrier gas flow. Carbon black is widely used as a reinforcing component in the production of rubbers and plastics. Tires use 70% of all carbon produced. It is produced in a furnace, by injecting raw hydrocarbon with nozzles into the stream of combustion products of natural gas (called heat-carrier gas), a spray jet is will be formed, accompanied by evaporation of raw materials, and pyrolysis in the end. It is important that the raw material is completely evaporated before pyrolysis begins, otherwise coke will form, contaminating the product. To improve the technology of carbon production, in particular, to ensure the complete evaporation of raw materials before the start of pyrolysis, it is impossible to do without mathematical modeling of the process itself. It is the most important way to obtain the most complete and detailed information about the features of the reactor. Such phenomena are usually modeled using multiphase flows.

1 Introduction

Carbon black is formed from oil-containing feedstock by heating it to about 950^{o}C. In this case, its cracking occurs with the formation of gas and powdered carbon black [1]. These components pass through filters that remove the carbon black. When water is added, the powder granulates. The granules are dried and conditioned. The resulting carbon black is used in the production of a wide variety of materials. But about 70% of all produced carbon is used in the production of pneumatic tires. The most difficult stage of the carbon production process is the injection of liquid hydrocarbon feedstock into the heat-carrier gas flow by nozzles in order to create the desired degree of atomization of the feedstock. The process of liquid atomization on real nozzles can occur with a wide range of liquid particle (droplet) sizes, liquid particle seeding density of the gas flow, and a significant uneven distribution of droplets in the gas flow. At the same time, it is necessary that the fineness of the atomization of the raw material, the uniformity of the distribution of droplets in the gas flow ensure its complete evaporation before the start of pyrolysis and the optimal structure of carbon black. Besides, the probability of formation of coke (grit), polluting the product, should be minimal [2]. The formulated requirements for the process of atomization and evaporation of raw materials in a heat-carrier gas flow can only be met if it is possible to conduct a three-dimensional numerical simulation of this process. It is numerical methods that will make it possible to better understand the structure of the flow and identify factors that affect the efficiency of spraying and evaporation of raw materials, and, consequently, the quality of the resulting carbon. A technique has been developed for numerical simulation of three-dimensional two-phase (heat-carrier gas and feedstock) and three-phase (heat-carrier gas, feedstock, and feedstock evaporation products) flows in a carbon black production reactor. The Eulerian models of multiphase flows based on the volume of fluid method (VOF) [3] implemented in the commercial software package (PC) ANSYS [4] are taken as a basis. Two VOF models of multiphase flows are considered and compared: two-phase model with an incompressible phase for raw materials and a compressible phase for gas; three-phase model with an incompressible phase for raw materials and evaporation products of raw materials and compressible phases for the gas. The reliability of the obtained results of numerical simulation is substantiated on the well-known problem of spraying a liquid jet under the influence of a gas flow, studied in detail experimentally [5] and numerically [6]. A method has been developed and numerically implemented for the formation of spray droplets according to the distribution of the volume fraction of raw materials in the flow area. An analysis of the droplet sizes was carried out and the Sauter mean diameter (SMD) of the spray, which is an important characteristic, was determined. The results of calculation of spraying and evaporation of raw materials in a reactor are presented.

2 Physical description of the problem

Carbon black can be manufactured using a reactor as shown in Fig. 1. In this reactor heat-carrier gas is flowing from its inlet, and into it by the nozzles the raw materials

are sprayed, the raw materials will breakup into droplets and evaporate eventually, and in the end, the pyrolysis process is conducted at the evaporated raw materials to produce the carbon black.

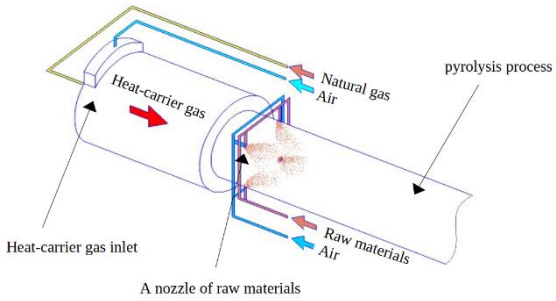

Fig. 1. Reactor for manufacturing carbon black

3 Multiphase flows models in ANSYS software

Multiphase flows are phenomena in which different flows (called phases) are interacting on each other at the same time. To describe the process of spraying and evaporation of liquid, there are several models in the ANSYS FLUENT software package as shown in Fig. 2.

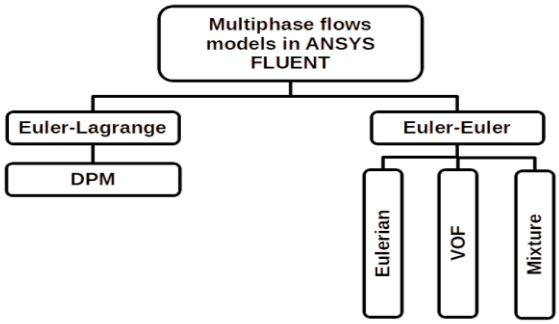

Fig. 2. Multiphase flows models in ANSYS FLUENT

The Euler-Euler models suits cases in which a distinct interface between the phases could be recognised, while Euler-Lagrange models more suitable for cases in which no distinct interface could be recognised (Fig. 3).

While injecting raw materials into the heat-carrier gas, a spray jet forms which makes Euler-Euler model better suited, but afterward the jet breaks up into droplets which makes Euler-Lagrange model better suited. Although The Eulerian model is the most general of all Euler-Euler models, it requires relatively much more computer resources than in VOF or mixture models, and by assuming the flow to be homogeneous (all the phases have the same velocity), the VOF model would be an efficient and accurate enough model to use.

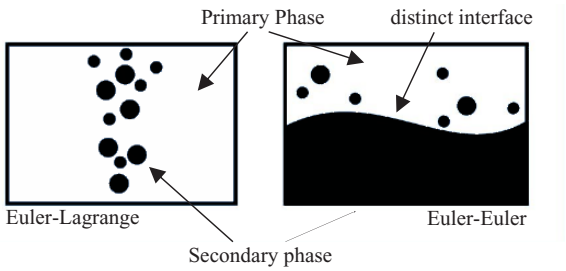

Fig. 3. Flow cases of Euler-Euler and Euler-Lagrange

4 The VOF model for two phases

In this model, the heat-carrier gas phase is compressible while the raw materials phases are incompressible. The volume of fraction equation is given by

$$\frac{\partial(\alpha_{raw})}{\partial t} + \nabla.(\alpha_{raw}u) = 0, \quad (1)$$

$$\rho = \alpha_{raw}\rho_{raw} + (1-\alpha_{raw})\rho_{gas}. \quad (2)$$

Here $\alpha_{raw}$is the volume fraction of raw materials, u is the velocity vector of the mixture, ρ_{raw}, ρ_{gas}, and ρ are the density of raw materials, heat-carrier gas, and mixture. The continuity equation for the mixture is given by

$$\frac{\partial\rho}{\partial t} + \nabla.(\rho u) = 0. \quad (3)$$

The conservation of momentum equation for the mixture

$$\frac{\partial}{\partial t}(\rho u) + \nabla.(\rho uu) = -\nabla p + \nabla.[\mu(\nabla u + \nabla u^T)] + \rho g + F_\sigma\,. \quad (4)$$

Here p is the pressure, μ is the viscosity of the mixture, and is calculated using the viscosities of raw materials μ_{raw} and heat-carrier gas μ_{gas} as following $\mu = \alpha_{raw}\mu_{raw} + (1-\alpha_{raw})\mu_{gas}$, g is the gravitational force, F_σ is the surface tension force

$$F_\sigma = \sigma\frac{\rho\kappa}{\frac{1}{2}(\rho_{raw}+\rho_{gas})}\nabla\alpha_{raw}. \quad (5)$$

Here κ is the interface curvature and calculated using the volume fraction of raw materials $\kappa = \nabla.\frac{\nabla\alpha_{raw}}{|\nabla\alpha_{Raw}|}$. The conservation of energy equation

$$\frac{\partial}{\partial t}(\rho E) + \nabla.\big(u(\rho E + p)\big) = \nabla.(k\nabla T). \quad (6)$$

Here E is the total energy of the mixture, T is the temperature of the mixture, k is the thermal conductivity of the mixture, and calculated using the thermal conductivity of the raw phase k_{raw}, and the heat-carrier gas phase k_{gas}, as following $k = \alpha_{raw}k_{raw} + (1-\alpha_{raw})k_{gas}$. The state equation of the heat-carrier gas phases

$$\rho_{gas} = \frac{pM_{gas}}{RT}. \quad (7)$$

Here M_{gas} is the molecular weight of heat-carrier gas, $R = 8.31\,\mathrm{J/(mol.K)}$ is the universal gas constant.

5 The VOF model for three phases

In this model we are considering three phases, one compressible (heat-carrier gas), and two incompressible (raw materials and the evaporation produced of raw materials). The volume of fraction equation is given by

$$\frac{\partial(\alpha_{raw})}{\partial t} + \nabla.(\alpha_{raw}u) = \dot{m}_{vapor,raw} - \dot{m}_{raw,vapor}, \quad (8)$$

$$\frac{\partial(\alpha_{vapor})}{\partial t} + \nabla.(\alpha_{vapor}u) = \dot{m}_{raw,vapor} - \dot{m}_{vapor,raw}, \quad (9)$$

$$\alpha_{gas} = 1 - \alpha_{raw} - \alpha_{vapor}. \quad (10)$$

Here α_{gas}, α_{vapor} are the volume fraction of heat-carrier gas and the evaporation produced of raw materials. $\dot{m}_{raw,vapor}$ is the volume fraction transfer from raw phase to the vapor phase, $\dot{m}_{vapor,raw}$ is the volume fraction transfer from vapor phase to the raw phase. The continuity equation for the mixture is given by

$$\frac{\partial\rho}{\partial t} + \nabla.(\rho u) = 0. \quad (11)$$

$$\rho = \alpha_{raw}\rho_{raw} + \alpha_{gas}\rho_{gas} + \alpha_{vapor}\rho_{vapor}. \quad (12)$$

The conservation of momentum equation for the mixture

$$\frac{\partial}{\partial t}(\rho u) + \nabla.(\rho uu) = -\nabla p + \nabla.[\mu(\nabla u + \nabla u^T)] + \rho g + F_\sigma . \quad (13)$$

Here the viscosity of the mixture $\mu = \alpha_{raw}\mu_{raw} + \alpha_{gas}\mu_{gas} + \alpha_{vapor}\mu_{vapor}$. The conservation of energy equation

$$\frac{\partial}{\partial t}(\rho E) + \nabla.\big(u(\rho E + p)\big) = \nabla.(k\nabla T). \quad (14)$$

Here the thermal conductivity of the mixture $k = k_{raw}\mu_{raw} + k_{gas}\mu_{gas} + k_{vapor}\mu_{vapor}$. The state equation of the heat-carrier gas phases

$$\rho_{gas} = \frac{pM_{gas}}{RT}. \quad (15)$$

Additional to equation (8)-(15), an evaporation-condensation model is needed to define the terms $\dot{m}_{raw,vapor}$ and $\dot{m}_{vapor,raw}$ in equations (8)-(9)

$$\text{if} T \geq T_{sat} \begin{cases} \dot{m}_{raw,vapor} = \lambda_c \alpha_{raw} \dfrac{(T - T_{sat})}{T_{sat}} \\ \dot{m}_{vapor,raw} = 0 \end{cases}, \quad (16)$$

$$\text{if} T < T_{sat} \begin{cases} \dot{m}_{vapor,raw} = \lambda_c \alpha_{raw} \dfrac{(T - T_{sat})}{T_{sat}} \\ \dot{m}_{raw,vapor} = 0 \end{cases}. \quad (17)$$

Here $\lambda_c = 0.01$ is a fitting parameter, T_{sat} is vaporization temperature.

6 Raw materials spray in a heat-carrier gas flow

To model the spray of raw materials into the heat-carrier gas, we will use the reactor shown in Fig. 4.

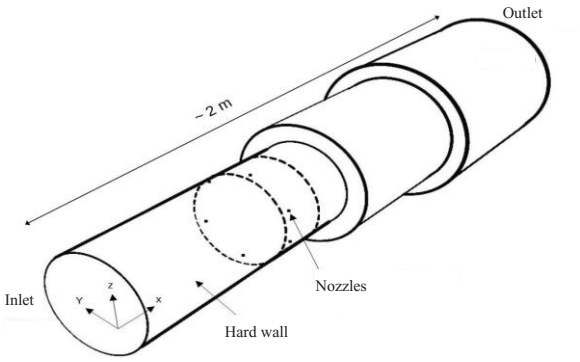

Fig. 4. Reactor for manufacturing carbon black

In this reactor we have six nozzles evenly spaced around the circumference in one section. Each nozzle has a diameter of 2.8 mm and through it raw materials flows at a rate of 0.6 m^3/h (each nozzle). The density of raw materials $\rho_{raw} = 1100\,Kg/m^3$, viscosity $\mu_{raw} = 0.055\,Kg/(m.s)$, thermal conductivity $k_{raw} = 0.6\,W/(m.s)$. The diameter of heat-carrier gas inlet is 280 mm and through it the gas flows at rate of 93697 m^3/h. The viscosity of the gas $\mu_{gas} = 6.91 \times 10^{-5}\,Kg/(m.s)$, thermal conductivity $k_{gas} = 0.0242\,W/(m.s)$, molecular weight $M_{gas} = 28.97 \times 10^{-3}\,Kg/mol$.

The difficulty with this reactor, is the huge difference in size of the nozzles comparing to the whole reactor. To use cells that is small enough for the nozzles, would results in a huge number of cells across the whole reactor. To get around this difficulty, a smaller geometry will be used as shown in Fig. 5.

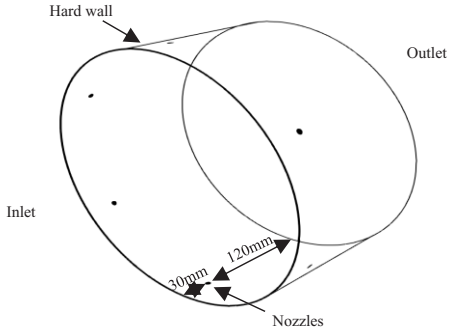

Fig. 5. A small segment from the reactor

The mesh in the cross section of the reactor around the upper nozzles is shown in Fig. 6.

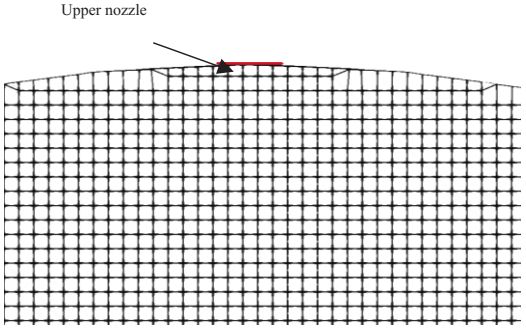

Fig. 6. The mesh around the upper nozzle

Both VOF model, the two-phases described in section 4 and the three-phases described in section 5, were applied to get the distribution of volume of fraction for raw materials. This distribution would give us an indication how raw materials are distributed along the reactor. Red colour represents high concentration of raw materials, while blue, low concentration. The distribution of volume of fraction for raw materials that resulted using the two-phases model is shown in Fig. 7 and Fig. 8.

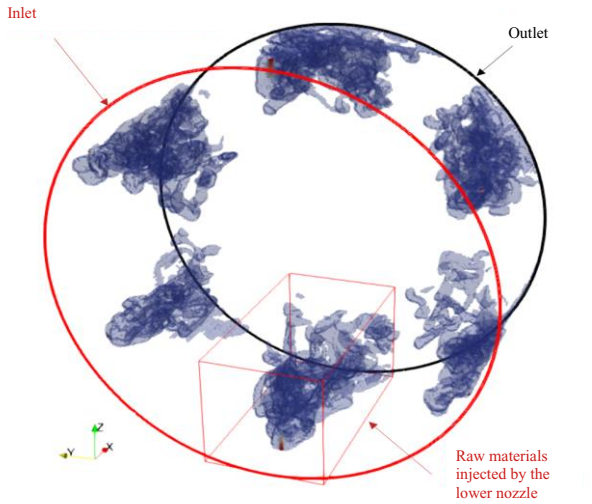

Fig. 7. Iso view for the distribution of volume fraction of raw materials (Two-phase)

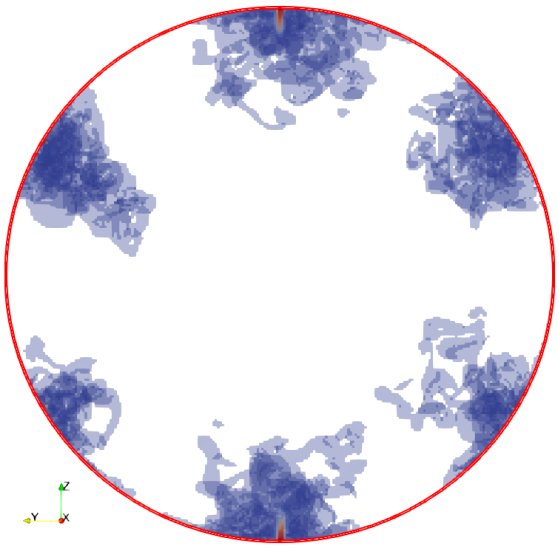

Fig. 8. Cross-section view for the distribution of volume fraction of raw materials (Two-phase)

The distribution of volume of fraction for raw materials that resulted using the three-phases model is shown in Fig. 9

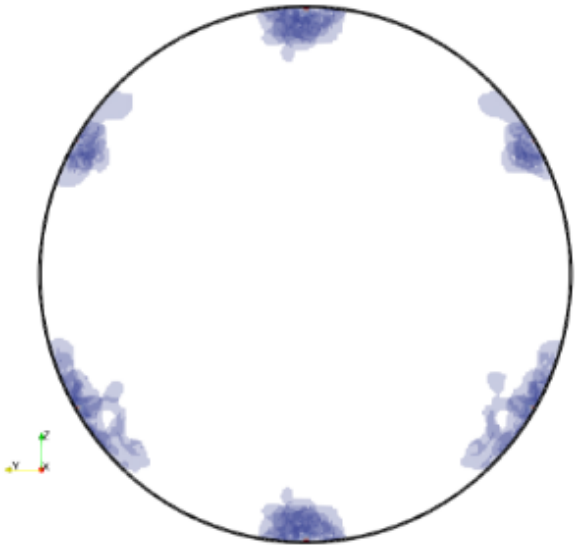

Fig. 9. Cross section view for the distribution of volume fraction of raw materials (Three-phase)

Comparing the distributions of volume fraction for raw materials, that resulted from both models: two-phases "no evaporation" (Fig. 8) and three-phases "with evaporation" (Fig. 9), we can see in Fig. 9 less concentration of raw materials than in Fig. 8. This shows the evaporation effect.

7 Dynamic adaptation of the mesh

It's been mentioned above that using cells small enough for the nozzles would results in a huge number of cells across the whole reactor, which is inefficient. A better way may be using adaptive meshes, in which refinement would occurs in regions with height gradient of volume fraction for raw materials. This will insure a much smaller number of cells and much smaller computer time. In ANSYS FLUENT the "Hanging node adaptation" is used to refine the mesh. Meshes produced by this method are characterized by nodes on edges and faces that are not vertices of all the cells sharing those edges or faces. During adaption, every cell in the mesh should be either refined, coarsened, or remain neutral. Back to reactor (Fig. 6), instead of using a cartesian mesh, an unstructured mesh shown in Fig. 10 is used, with a space step of 10 mm and an initial refinement near the nozzles. The reason for using an unstructured mesh with bigger space step is to reduce the number of cells, knowing that the space steps will get smaller as refinement occurs with time, which ensures the required accuracy. The reason behind the initial refinement of the cells near the nozzles is to insure the continuation of refinement from that region (the nozzles) and so forth.

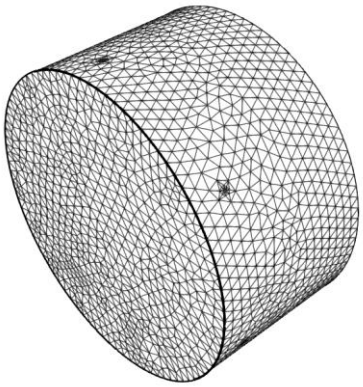

Fig. 10. Unstructured mesh

The adaptation algorithm is as follows: for every cell in the mesh if $0 \leq \frac{\nabla(\alpha_{raw})}{\max|\nabla(\alpha_{raw})|} \leq 0.1$ it's marked for coarsening, if $0.1 < \frac{\nabla(\alpha_{raw})}{\max|\nabla(\alpha_{raw})|} < 0.11$ it's remain neutral, if $0.11 \leq \frac{\nabla(\alpha_{raw})}{\max|\nabla(\alpha_{raw})|} \leq 1$ it's marked for refinement. The gradient of volume fraction of raw material α_{raw} equals to zero inside heat-carrier gas and raw materials zones, and bigger than zero only at the interface between these two phases. This algorithm will insure to refine the cells that contain the interface, and coarsen the rest. Fig. 11 shows the development of the mesh and the distribution of volume fraction of raw materials while using adaptation and the VOF model.

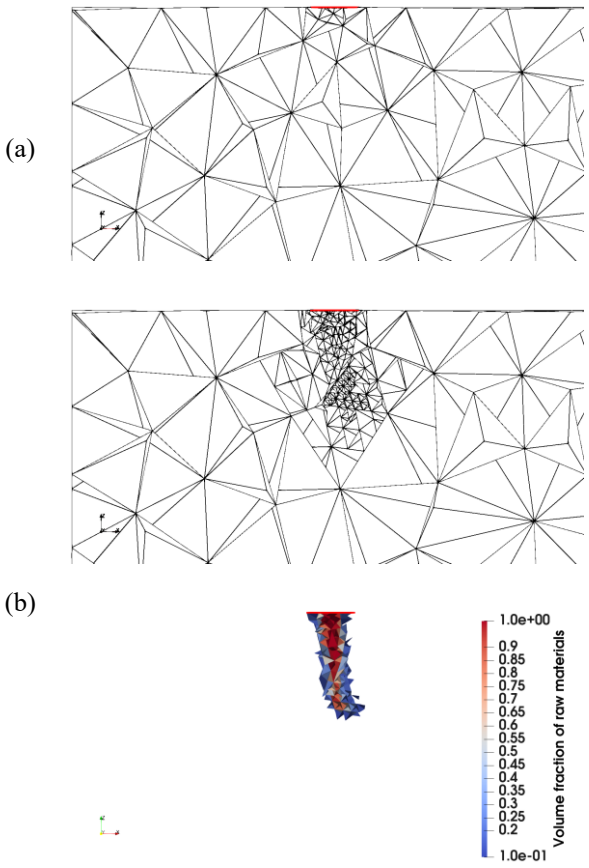

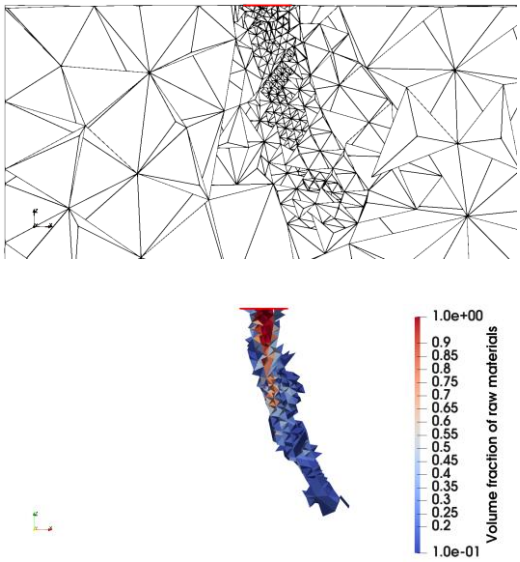

Fig. 11. The mesh and the distribution of volume fraction of raw material at $t = 0$ (a); $t = 4 \cdot 10^{-4}$s (b); $t = 9 \cdot 10^{-4}$s (c)

Fig. 12 shows all six spray jets. Comparing between the volume of fraction distributions resulted of using cartesian mesh (Fig. 12) and adaptive mesh (Fig. 8), we can notice that using the adaptive mesh captured the main bulk of the spray jet better than in cartesian mesh, but failed to capture the cloud around the jet. This is due to the large cells volume relative to the small values for volume fraction of raw materials $< 10^{-3}$ in these zones.

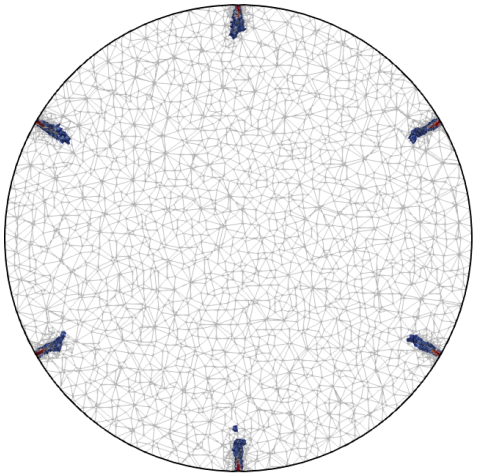

Fig. 12. Cross-section view for the distribution of volume fraction of raw materials

8 Droplets formation and SMD

It is known that the main jet breaks up into droplets, and these droplets in turn breaks up into smaller one and so on until it atomized and evaporated as shown in Fig. 13. The VOF models, described earlier, show the distribution of volume of fractions of raw materials. Unless the cells are small enough (which is inefficient in our case) it would not be useful to observe any droplets, we will only get a cloud similar to Fig. 8.

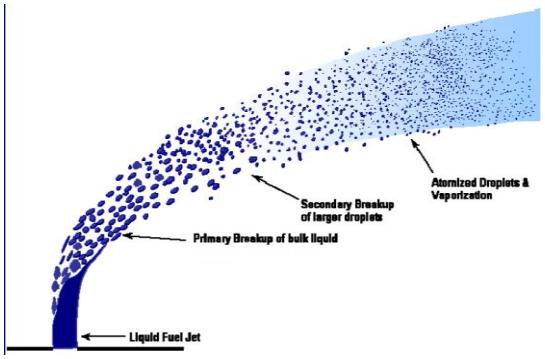

Fig. 13. Typical spray jet

As an attempt to solve this difficulty an algorithm was developed to form the droplets. It takes the distribution of volume fraction of raw materials as input, and returns the locations and sizes of the droplets as output. The main idea of the algorithm is that each droplet has a local maximum in the distribution of the raw material volume fraction, hence, the distribution is checked, and if a local maximum is found, it will be grouped with all neighbouring cells (having a decreasing value of the volume fraction). This group is then identified as one droplet. The algorithm generates N droplets, each of them is a set of n_i cells. The center of droplet i is

$$x_i = \frac{1}{A_i}\sum_{j=1}^{n_i}\frac{(\alpha_{raw})_j}{(n_d)_j}(x_c)_j\,, \tag{18}$$

$$y_i = \frac{1}{A_i}\sum_{j=1}^{n_i}\frac{(\alpha_{raw})_j}{(n_d)_j}(y_c)_j\,, \tag{19}$$

$$z_i = \frac{1}{A_i}\sum_{j=1}^{n_i}\frac{(\alpha_{raw})_j}{(n_d)_j}(z_c)_j\,. \tag{20}$$

Here $(\alpha_{raw})_j$ is the volume fraction of raw materials of cell j, $(n_d)_j$ is the number of droplets containing the cell j, $(x_c)_j$, $(y_c)_j$, $(z_c)_j$ is the center of cell j $A_i = \sum_{j=1}^{n_i}\frac{(\alpha_{raw})_j}{(n_d)_j}$. The volume of droplet i is

$$V_i = \sum_{j=1}^{n_i}\frac{\alpha_j}{(n_d)_j}(V_c)_j\,. \tag{21}$$

In (20) $(V_c)_j$ is the volume of cell j. Considering all the droplets are of a spherical shape, the radius of droplet i is

$$R_i = \sqrt[3]{\frac{3}{4\pi}V_i}. \tag{22}$$

By applying the algorithm on a distribution of volume fraction of raw materials as shown in Fig. 14 will get the locations of the droplets and their sizes as shown in Fig. 15.

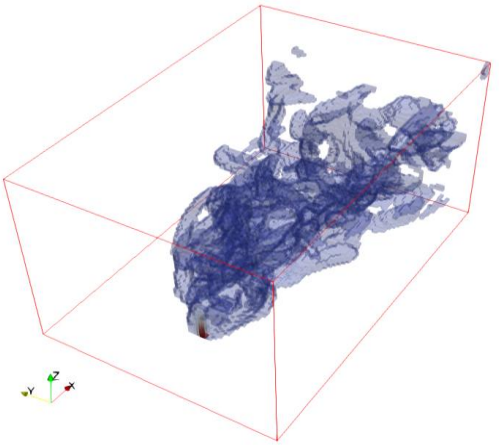

Fig. 14. The distribution of volume of fraction for raw materials near the lower nozzle (algorithm input)

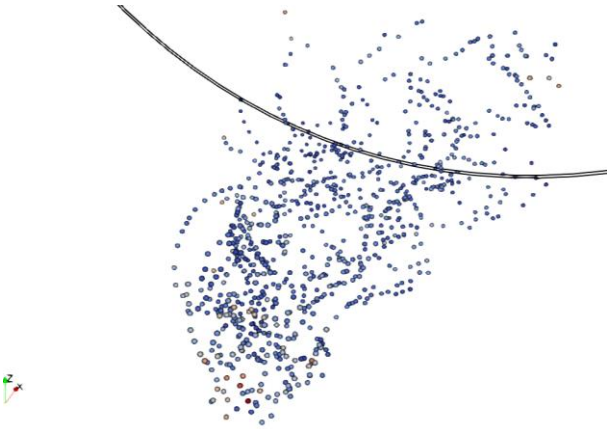

Fig. 15. Droplets location and size (algorithm output)

To characterize the droplets, the Sauter mean diameter $D_{3,2}$ is used

$$D_{32} = \frac{6.V_{\text{total}}\ (\text{the volume of all drops})}{S_{\text{total}}\ (\text{Surface area of all droplets})} \tag{23}$$

In Fig. 16, the relation between $D_{3,2}$ and time is plotted. It shows a convergence of $D_{3,2}$ over time.

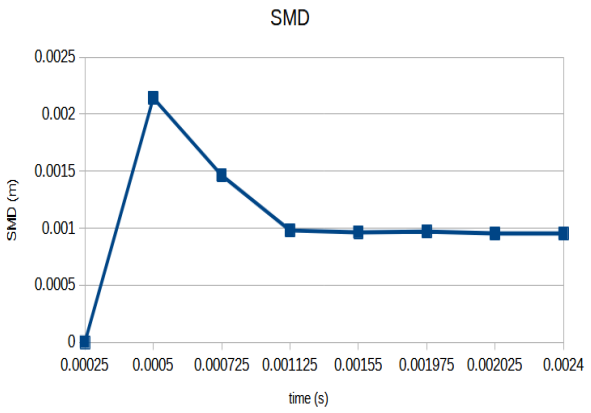

Fig. 16. Sauter mean diameter $D_{3,2}$

9 Conclusions

To better understand carbon black production process, it is necessary to have a numerical model that simulates the spray jet of raw materials (hydrocarbons) into heat-carrier gas (the stream of combustion products of natural gas). This model on one hand should be accurate, and on the other hand, should be efficient in terms of computer resources requirements.

Spray jets of liquid into gas is usually simulated using multiphase models in which phases interact with each other. Some models are represented in ANSYS FLUENT, some are more suited to one case than others, and some are more general but requires more computational resources. For the Spary jet of raw materials of carbon black, the Euler-Euler models would be better suited, but afterwards when the jet breaks up into droplets, the Euler-Lagrange models would be better suited. By assuming the phases to be homogenous, we can notably reduce the calculation efforts by using the VOF model instead of the Eulerian. This what makes the VOF model an efficient and accurate enough model for the task.

Two cases using the VOF model were considered and compared: a two-phase model with an incompressible phase for raw materials and a compressible phase for gas; three-phase model with an incompressible phase for raw materials and the evaporation products of raw materials, and a compressible phase for gas. Comparison between the models shows the notable effect of the evaporation.

Cells of the mesh are the major factors when it's comes to efficiency and accuracy. The starting reactor geometry (Fig. 4) has a huge difference in size of the nozzles comparing to the whole reactor size, so using cells small enough for the nozzles would results in a huge number of cells across the whole geometry. Using a smaller geometry (the small section around the nozzles, Fig. 5) would enormously reduce the number of irrelevant cells. Furthermore, using adaptive meshes in which refinement would occurs when and where it’s needed, would ensures much smaller number of cells and better capture the main bulk of the spray jet, but would fail to capture the cloud around the jet.

The VOF models only shows the distribution of volume of fractions of raw materials, but unless the cells are small enough (which is inefficient in our case) it would not be useful to observe any droplets, we will only get a cloud similar to Fig. 8. To solve this problem an algorithm was developed. It takes the distribution of volume fraction of raw materials as input, and returns the locations and sizes of the droplets as output. Using the algorithm's output, the convergence of Sauter mean diameter $D_{3,2}$ with time was shown.

References

1. T.G. Gulmisaryan, V.M. Kapustin, I.P. Levenberg, Carbon Black: Morphology, Property, Production (Kauchuk i Rezina, Moscow, 2017)
2. V. Y Orlov, A.M. Komarov, L.A. Lyapina, Production and Use of Carbon Black for Rubber (Alexander Rutman, Yaroslavl, 2002)
3. C.W. Hirt, B.D. Nichols, *Volume of fluid (VOF) method for the dynamics of free boundaries,* J. Comp. Physics **39,** 201 (1981)
4. N.N. Fedorova, S.A. Valger, Y.V. Zakharova, Modeling of hydro-gasdynamic processes in ANSYS 17.0 PC (NGASU (Sibstrin), Novosibirsk, 2016)
5. P.K. Wu, K.A. Kirkendall, R.P. Fuller, A.S. Nejad, *Spray structures of liquid jets atomized in subsonic crossflows,* J. Propul. Power **14,** 173 (1998)
6. A.M. Sipatov, S.A. Karabasov, L.Y. Gomzikov, T.V. Abramchuk, G.N. Semakov, *Modeling the spray process using adaptive grid models*, Computational Continuum Mechanics, 93 (2015)